

## Length scale for the superconducting Nernst signal above $T_c$ in $\text{Nb}_{0.15}\text{Si}_{0.85}$

A. Pourret,<sup>1</sup> H. Aubin,<sup>1</sup> J. Lesueur,<sup>1</sup> C. A. Marrache-Kikuchi,<sup>2</sup> L. Bergé,<sup>2</sup> L. Dumoulin,<sup>2</sup> and K. Behnia<sup>1</sup>

<sup>1</sup>*Laboratoire de Physique Quantique (CNRS), ESPCI, 10 Rue de Vauquelin, 75231 Paris, France*

<sup>2</sup>*CSNSM, IN2P3-CNRS, Bâtiment 108, 91405 Orsay, France*

(Received 11 September 2007; published 12 December 2007)

We present a study of the Nernst effect in amorphous superconducting thin films of  $\text{Nb}_{0.15}\text{Si}_{0.85}$ . The field dependence of the Nernst coefficient above  $T_c$  displays two distinct regimes separated by a field scale set by the Ginzburg-Landau correlation length (CL). A single function  $F(\xi)$ , with the CL as its unique argument set either by the zero-field CL (in the low magnetic field limit) or by the magnetic length (in the opposite limit), describes the Nernst coefficient. We conclude that the Nernst signal observed on a wide temperature ( $30 \times T_c$ ) and field ( $4 \times B_{c2}$ ) range is exclusively generated by short-lived Cooper pairs.

DOI: [10.1103/PhysRevB.76.214504](https://doi.org/10.1103/PhysRevB.76.214504)

PACS number(s): 74.70.Tx, 71.27.+a, 72.15.Jf

### INTRODUCTION

The observation of a finite Nernst signal in the normal state of high- $T_c$  cuprates<sup>1</sup> has revived interest in the study of superconducting fluctuations. In conventional superconductors, short-lived Cooper pairs above  $T_c$  have been mostly examined through the phenomena of paraconductivity<sup>2</sup> and fluctuation diamagnetism.<sup>3</sup> Due to a sizeable contribution from free electrons to conductivity and magnetic susceptibility, the sensitivity of these probes to superconducting fluctuations is limited to a narrow region close to  $T_c$ .<sup>4</sup> Because of a low superfluid density, the superconducting state in underdoped cuprates is particularly vulnerable to phase fluctuations.<sup>5</sup> Therefore, long-lived Cooper pairs without phase coherence and vortexlike excitations are considered as the main source of the anomalous Nernst effect observed in an extended temperature window above  $T_c$  in underdoped cuprates.<sup>1</sup>

In a recent experiment on amorphous thin films of the conventional superconductor  $\text{Nb}_{0.15}\text{Si}_{0.85}$ ,<sup>6</sup> a Nernst signal generated by short-lived Cooper pairs could be detected up to very high temperatures ( $30 \times T_c$ ) and high magnetic field ( $4 \times B_{c2}$ ) in the normal state. In these amorphous films, the contribution of free electrons to the Nernst signal is negligible. Indeed, the Nernst coefficient of a metal scales with electron mobility.<sup>7</sup> The extremely short mean free path of electrons in amorphous  $\text{Nb}_{0.15}\text{Si}_{0.85}$  damps the normal-state Nernst effect and allows a direct comparison of the data with theory. In the zero-field limit and close to  $T_c$ , the magnitude of the Nernst coefficient was found to be in quantitative agreement with a theoretical prediction<sup>8</sup> by Ussishkin, Sondhi, and Huse (USH), invoking the superconducting CL as its single parameter. At high temperature and finite magnetic field, the data were found to deviate from the theoretical expression.

In this paper, we present a set of measurements yielding an extensive set of data up to fields and temperatures exceeding  $T_c$  and  $H_{c2}$  by one order of magnitude. We present a detailed analysis, upgrading the initial report on the agreement between the results with the USH theoretical expression. In our data, Nernst coefficient,  $\nu$ , is reduced as one increases either the temperature or the magnetic field. We show here that both these variations reflect a unique depen-

dence on a single length scale. A striking visualization of this emerges when one substitutes temperature and magnetic field by their associated length scales: The zero-field superconducting CL  $\xi_d(T)$  and the magnetic length  $l_B(B) = (\hbar/2eB)^{1/2}$ . The symmetric contour lines of  $\nu$  in the  $(l_B, \xi_d)$  plane shows that its dependence on both field and temperature can be described by a single function with the superconducting CL  $\xi$  as its unique argument. In the low-field limit, the CL is set by  $\xi_d$  and in the high-field limit by  $l_B$ . In the intermediate regime, when  $\xi_d \approx l_B$ , the CL is a simple combination of these two lengths. This observation is additional proof that the Nernst signal observed up to high temperature ( $30 \times T_c$ ) and high magnetic field ( $4 \times B_{c2}$ ) in this system is exclusively generated by superconducting fluctuations—i.e., short-lived Cooper pairs. Hence the functional dependence of the Nernst coefficient on the CL is empirically determined in a wide range extending from the long CL regime, where the data follow the prediction of USH theory, to the short CL regime, where the Ginzburg-Landau approximation fails and no theoretical expression is yet available.

### EXPERIMENTAL

Amorphous  $\text{Nb}_x\text{Si}_{1-x}$  thin films were prepared as described previously<sup>9,11</sup> and are believed to be clusters-free. AFM microscopy on films as thin as 2.5 nm (Ref. 12) did not find any indications of clusters. Moreover, the superconducting transition temperature (decreasing as the films become thinner) remains sharp, with no indications of any secondary superconducting phase at any temperature in the resistivity measurements.<sup>11</sup> This indicates that our samples are homogeneously disordered. This conclusion is corroborated by a TEM study<sup>13</sup> showing that only  $\text{Nb}_x\text{Si}_{1-x}$  alloys annealed at 500 °C present Nb-rich clusters. We also checked the stability of the samples with respect to temperature cycling and time. The resistivity of the samples, kept at room temperature several months after their preparation, showed a change of the order of 1 percent on a six months time scale, in rough agreement with a recent study.<sup>14</sup> This small time dependence of resistivity is not surprising given the glassy nature of the system under study. The competition between superconducting, metallic and insulating ground states is controlled by the Nb concentration, the thickness of the films, or the magnetic

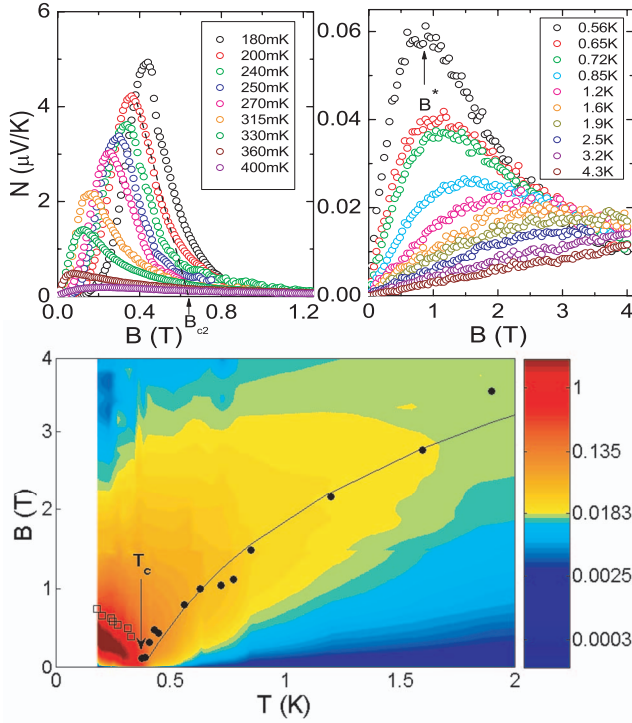


FIG. 1. (Color) Nernst signal ( $N$ ) as a function of magnetic field for temperatures ranging from 0.180 K to 0.360 K (upper left panel) and from 0.56 to 4.3 K (upper right panel) measured on sample 2 ( $T_c=380$  mK). Above (below)  $T_c$  the position of the maximum in the field dependence of the Nernst signal increases (decreases) with decreasing temperature. Lower panel: Logarithmic color map of the Nernst signal in the  $(B, T)$  plane. Superimposed on the plot are the values of the critical field (open squares), below  $T_c$ , and  $B^*$  (full circles), above  $T_c$ . Note the symmetric evolution of these two field scales with respect to  $T_c$ . The continuous line is the field scale set by the Ginzburg-Landau CL,  $B^* = \phi_0/2\pi\xi_d^2$ .

field.<sup>9–11</sup> Two samples of identical stoichiometry— $\text{Nb}_{0.15}\text{Si}_{0.85}$ —but with different thicknesses and  $T_c$  are used in this study. Sample 1 (2) was 12.5 (35) nm thick and its midpoint  $T_c$  was 0.165(0.380) K. The physical properties of these two samples as well as the experimental setup were detailed in our previous communication, which also presented part of the data discussed here.<sup>6</sup>

## DISCUSSION

Figure 1 shows the Nernst signal,  $N=E_y/(-\nabla_x T)$  as a function of magnetic field and temperature, for sample 2. Below  $T_c$ , the magnetic field dependence shows the characteristic features of vortex-induced Nernst effect, well known from previous studies on conventional superconductors<sup>15</sup> and high- $T_c$  cuprates.<sup>1</sup> For each temperature, the Nernst signal increases steeply when the vortices become mobile following the melting of the vortex solid state. It reaches a maximum and decreases at higher fields when the excess entropy of the vortex core is reduced. As the temperature decreases the position of this maximum shifts towards higher magnetic fields. This is not surprising since all field scales associated with superconductivity are expected to increase with decreasing

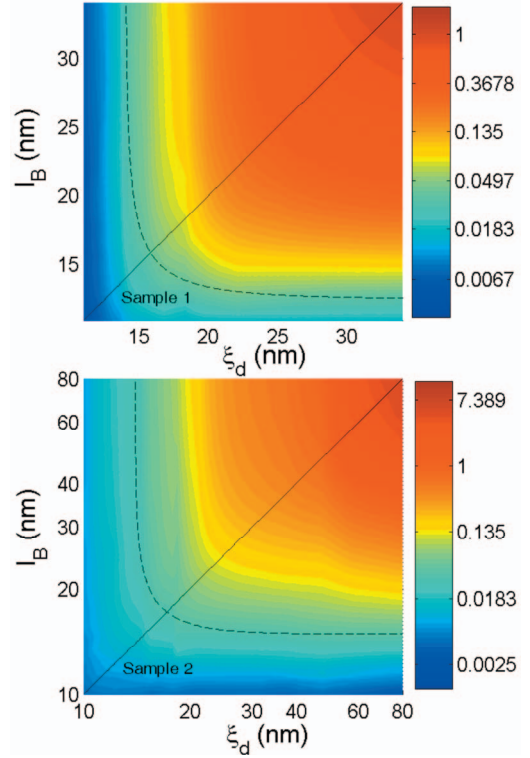


FIG. 2. (Color) Logarithmic color map of the Nernst coefficient as a function of the magnetic length  $l_B$  and the zero-field CL  $\xi_d$  for sample 1 (upper panel) and sample 2 (lower panel). Note the symmetry of the Nernst coefficient with respect to the diagonal continuous line ( $l_B=\xi$ ). Dots lines represents contours for  $\xi=15$  nm with  $\xi=[1/\xi_d^4+1/(c\times l_B)^4]^{-1/4}$ .  $c=1.12$  for sample 1 and  $c=0.93$  for sample 2.

temperature. In particular, this is the case of the upper critical field,  $B_{c2}$ , which can be roughly estimated by a linear extrapolation of the Nernst signal to zero as it has been done in cuprates.<sup>1</sup>

Above  $T_c$ , the temperature dependence of the characteristic field scale is reversed. At low magnetic field, the Nernst signal  $N=R_{\text{square}}\times\alpha_{xy}$  increases linearly with field, as expected from the USH theory where  $\alpha_{xy}$  follows the simple expression<sup>8</sup>

$$\alpha_{xy} = \frac{1}{12\pi} \frac{k_B e}{\hbar} \frac{\xi^2}{l_B^2}. \quad (1)$$

[Note that here we use the definition of  $l_B(B)=(\hbar/2eB)^{1/2}$ , which differs by a factor of  $\sqrt{2}$  from what was used in Refs. 8 and 6]. Upon increasing the magnetic field, the Nernst signal deviates from this linear field dependence, reaches a maximum at a field scale  $B^*$  and decreases afterwards to a weakly temperature-dependent magnitude. In contrast to the superconducting state ( $T<T_c$ ), the position of the maximum shifts to higher fields with increasing temperature. The contour plot in the  $(T, B)$  plane (lower panel) shows that these two field scales,  $B_{c2}$  and  $B^*$ , evolve symmetrically with respect to the critical temperature. One major observation here is that the magnitude and the temperature dependence of  $B^*$

follows the field scale set by the Ginzburg-Landau CL  $\xi_d = \xi_{0d}/\sqrt{\epsilon}$  through the relation  $B^* = \phi_0/2\pi\xi_d^2$  where  $\phi_0$  is the flux quantum and  $\epsilon = \ln(T/T_c)$  the reduced temperature. (This field scale was dubbed “the ghost critical field” by Kapitulinik and co-workers.<sup>16</sup>) The value for the CL at zero-temperature  $\xi_{0d}$  is determined from the BCS formula in the dirty limit  $\xi_{0d} = 0.36\sqrt{(3/2)(\hbar v_F \ell / k_B T_c)}$ , where  $v_F \ell = 4.35 \times 10^{-5} \text{ m}^2 \text{ s}^{-1}$  is estimated using the known values of electrical conductivity and specific heat.<sup>6</sup> Thus the decrease of the Nernst signal at the field scale  $B^*$  is the consequence of the reduction of CL when the cyclotron diameter  $l_B$  becomes shorter than the zero-field CL  $\xi_d$ , at a given temperature. This phenomena is well known from studies of fluctuations diamagnetism in low temperature superconductors<sup>3</sup> and cuprates.<sup>17</sup> While in the low field limit, the magnetic susceptibility should be independent of the magnetic field—i.e., in the Schmid limit<sup>18</sup>—the magnetic susceptibility is experimentally observed to decrease with the magnetic field, following the Prange’s formula,<sup>19</sup> which is an exact result within the Ginzburg-Landau formalism that takes into account the reduction of the CL by the magnetic field. In this regime, the amplitude fluctuations are described as evanescent Cooper pairs arising from free electrons with quantized cyclotron orbits.<sup>4</sup> In our experiment, we can clearly distinguish the low-field limit—where the cyclotron length is larger than the CL—from the high-field limit, where the CL has been reduced from its value at zero field to a shorter value given by the magnetic length.

Figure 2 presents a contour plot (with a logarithmic scale of the colors) of the Nernst coefficient  $\nu = N/B$  in the  $(l_B, \xi_d)$  plane. When  $l_B > \xi_d$ , the contour lines are parallel to the magnetic length axis, meaning that the Nernst coefficient depends only on  $\xi_d$ . When  $l_B < \xi_d$ , the contour lines are parallel to the CL axis, meaning that the Nernst coefficient depends only on  $l_B$ . Furthermore, in both samples, the contour lines are almost symmetric with respect to the  $l_B = \xi_d$  line. In other words, the Nernst coefficient appears to be uniquely determined by the CL, no matter whether  $\xi_d$  or  $l_B$  sets it.

Therefore, we are entitled to assume that there exists a function which links  $\nu$  to the CL. In the zero-field limit, the latter is set by  $\xi_d$ , and we can empirically extract from our data a function  $F(\xi)$  such as  $F(\xi) = \alpha_{xy}/B = (\nu/R_{\text{square}})(T, B \rightarrow 0)$ . This function is shown in Fig. 3 (upper panel). For large  $\xi$ , it is proportional to  $\xi^2$ , in agreement with the USH expression. For small  $\xi$ , however, we find that this function becomes roughly proportional to  $\xi^4$ . Now a remarkable observation follows: When this function  $F(\xi)$  is plotted with the magnetic length  $l_B$  as argument, as shown in the lower panel of Fig. 3, we find that it almost describes the magnitude and the field dependence of the Nernst coefficient at high magnetic field. This demonstrates that in these two opposite limits, ( $\xi \approx \xi_d$  and  $\xi \approx l_B$ ), the Nernst coefficient is determined by this single function  $F(\xi)$  that depends uniquely on the CL.

This function, extracted from the zero field data and observed to describe the data at high magnetic field, should also be valid at intermediate field, when  $\xi_d \approx l_B$ . In this intermediate region, with the increasing magnetic field, the CL progressively evolves from  $\xi_d$  to  $l_B$ . A simple relation for  $\xi$  that verifies the conditions,  $\xi \approx \xi_d$  when  $l_B \rightarrow \infty$ , and  $\xi \approx c \times l_B$  when  $l_B \rightarrow 0$  is given by

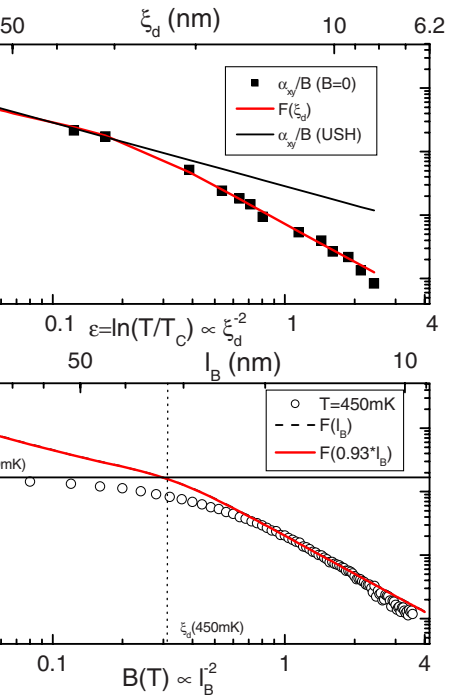


FIG. 3. (Color online) Upper panel: The transverse Peltier coefficient  $\alpha_{xy}$  divided by the magnetic field  $B$  (black squares) as a function of the reduced temperature  $\epsilon$  (bottom axis) and CL (top axis) for-sample 2 on a log-log scale. At low  $\epsilon$ , the experimental data are consistent with the USH model (solid line). The function  $F(\xi)$  shown as a red line is a fit to the data. Lower panel: The same function, (dot-line) plotted using  $l_B$  as its argument,  $F(l_B)$ , as a function of the magnetic field (bottom axis) and  $l_B$  (top axis). Note that it is consistent with the magnitude and field dependence of the data acquired at high magnetic field. The function  $F(c \times l_B)$  (continuous line) describes nicely the data when  $c=0.93$ . At low magnetic field, when  $l_B > \xi_d$ , the data deviates from  $F(c \times l_B)$  to reach the field-independent value  $F(\xi_d)$ .

$$\frac{1}{\xi^\gamma} = \frac{1}{\xi_d^\gamma} + \frac{1}{(c \times l_B)^\gamma}, \quad (2)$$

where the prefactor  $c$  and the exponent  $\gamma$  are to be determined from the experimental data. The prefactors  $c=1.12$  for sample 1 and  $c=0.93$  for sample 2 are determined such as  $F(c \times l_B)$  gives precisely the field dependence of the Nernst coefficient at high magnetic field, shown Fig. 3. The slight difference between the prefactors for the two samples is not understood at this stage. It appears to be larger than the experimental margin of error and suggests that other parameters not taken into account in this analysis may be involved, such as the thickness of the samples. To get the value of the exponent  $\gamma$ , we first note that the curves  $[\alpha_{xy}/B(B, T)]/[\alpha_{xy}/B(B \rightarrow 0, T)]$ , for temperature  $T > 2 \times T_c$ , collapse on a unique curve when they are plotted as a function of  $\xi_d/l_B$ , as shown Fig. 4. Then, using  $F(\xi) \sim \xi^4$ —as previously observed for  $T > 2 \times T_c$ —and using Eq. (2), we find that  $F(\xi)/F(\xi_d) = [1 + (\xi_d/c \times l_B)^\gamma]^{-4/\gamma}$  depends only on the ratio  $\xi_d/l_B$ , and so has the appropriate functional form to describe the collapsed data. For both samples, the best fit is

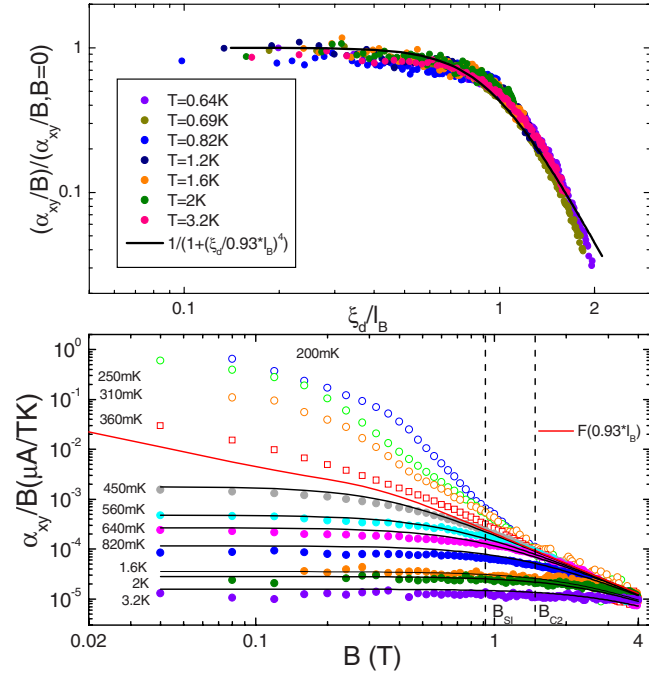


FIG. 4. (Color online) Upper panel:  $\alpha_{xy}/B$  normalized to its zero-field value vs  $\xi_d/l_B$  for sample 2. All the data at temperatures between 430 mK and 3.2 K are shown here to collapse on  $1/[1+(\xi_d/0.93 * l_B)^4]$  (thick line). Lower panel:  $\alpha_{xy}/B$  as a function of  $B$  for temperatures ranging from 200 mK to 3.2 K on a log-log scale. The function  $F(\xi)=(\alpha_{xy}/B)(\xi_d)$  extracted from the data at zero field is plotted here as a function of  $l_B$  (thick red line). At high magnetic field, all the data, above and below  $T_c$  tend towards  $F(c \times l_B)$ . Note that  $F(c \times l_B)$  is the separatrix of the data above and below  $T_c$ . Also shown is  $F(\xi)$  for several values of  $\xi_d$  corresponding to different temperatures, and plotted as function of  $\xi=[1/\xi_d^4+1/(0.93 * l_B)^4]^{-1/4}$ .

obtained when  $\gamma=4$ , as shown Fig. 4 for sample 2. Such a value of  $\gamma$  implies that the first nonlinear correction to the field dependence of  $\alpha_{xy}$  is proportional to  $B^2$  (i.e.,  $l_B^{-4}$ ), in agreement with analyticity arguments.<sup>22</sup> With these parameters just determined, Fig. 2 shows that the contour lines of equal Nernst coefficient can be described by curves of constant CL  $\xi$  as given by Eq. (2). Thus, as shown Fig. 4, above  $T_c$ , the magnitude of the Nernst coefficient at any temperature and magnetic field is given by this unique function

$F(\xi)=(\alpha_{xy}/B)(\xi)$ , determined experimentally at zero field, where the CL is given by Eq. (2).

Figure 4 also shows that the magnitude and field dependence of the Nernst signal, measured for temperatures  $T < T_c$  and high magnetic field ( $B > B_{c2}$ ), can also be described by  $F(c \times l_B)$ . In particular, we see that the Nernst data measured at a temperature close to  $T_c$  follow closely the curve  $F(c \times l_B)$  on a wide magnetic field range; this is expected for the diverging Ginzburg-Landau CL when approaching  $T_c$ . It is remarkable to note that the curve  $F(\xi)$ , extracted from the data at zero-field, and plotted as a function of  $l_B$ , gives precisely the separatrix between the curves  $(\alpha_{xy}/B)(B)$  measured above and below  $T_c$ . Below  $T_c$ ,  $\alpha_{xy}/B$  joins the function  $F(c \times l_B)$  at the upper critical field  $B_{c2} \approx 1.5T$ , which is larger than the critical field of the superconductor-insulator transition,  $B_{SI}=0.91T$ , defined as the crossing field of  $R(B)$  curves.<sup>11</sup>

The overall consistency of this analysis demonstrates that  $\alpha_{xy}$  is set by  $\xi_d$  over a wide temperature range ( $30 \times T_c$ ).<sup>21</sup> As noticed previously, when  $\xi_d$  is large,  $\alpha_{xy}$  is consistent with USH expression. However, below a CL of the order of  $\xi_{0d}$ , it deviates downward from the USH formula. Such a deviation is actually expected for theories based on the Ginzburg-Landau formalism, which are known to overestimate the effect of short-wave length fluctuations.<sup>4</sup>

## CONCLUSION

Let us conclude by briefly commenting the case of cuprates. One crucial issue to address is the existence of the “ghost critical field” detected here. We note that such a field scale has not been identified in the analysis of the cuprate data.<sup>1</sup> However, one shall not forget that the normal state of the underdoped cuprates is *not* a simple dirty metal. The contribution of normal electrons to the Nernst signal is too large to be entirely negligible. This makes any comparison between theory and data less straightforward than the analysis performed here. Moreover, in  $\text{Nb}_{0.15}\text{Si}_{0.85}$  there is a single temperature scale,  $T_{BCS}$ , for the destruction of superconductivity. In contrast, the situation in the cuprates may be complicated by the possible existence of two distinct temperature scales: The pairing temperature and a Kosterlitz-Thouless-like temperature leading to a phase-fluctuating superconductor.<sup>20</sup>

<sup>1</sup>Y. Wang, L. Li, and N. P. Ong, Phys. Rev. B **73**, 024510 (2006).

<sup>2</sup>R. E. Glover, Phys. Lett. **25A**, 542 (1967).

<sup>3</sup>J. P. Gollub, M. R. Beasley, R. Callarot, and M. Tinkham, Phys. Rev. B **7**, 3039 (1973).

<sup>4</sup>W. J. Skocpol and M. Tinkham, Rep. Prog. Phys. **38**, 1049 (1975).

<sup>5</sup>V. J. Emery and S. A. Kivelson, Nature (London) **374**, 434 (1995).

<sup>6</sup>A. Pourret, H. Aubin, J. Lesueur, C. Marrache-Kikuchi, L. Berge, L. Dumoulin, and K. Behnia, Nat. Phys. **2**, 683 (2006).

<sup>7</sup>K. Behnia, M. A. Measson, and Y. Kopelevich, Phys. Rev. Lett. **98**, 076603 (2007).

<sup>8</sup>I. Ussishkin, S. L. Sondhi, and D. A. Huse, Phys. Rev. Lett. **89**, 287001 (2002).

<sup>9</sup>S. Marnieros, L. Berge, A. Juillard, and L. Dumoulin, Phys. Rev. Lett. **84**, 2469 (2000).

<sup>10</sup>H. L. Lee, J. P. Carini, D. V. Baxter, W. Henderson, and G. Gruner, Science **287**, 633 (2000).

<sup>11</sup>H. Aubin, C. A. Marrache-Kikuchi, A. Pourret, K. Behnia, L. Berge, L. Dumoulin, and J. Lesueur, Phys. Rev. B **73**, 094521

- (2006).
- <sup>12</sup>C. Marrache-Kikuchi, Ph.D. thesis, Orsay, 2006.
- <sup>13</sup>D. Querlioz, D. R. Queen, and F. Hellman, *Appl. Phys. Lett.* **87**, 221901 (2005).
- <sup>14</sup>B. Baek, P. D. Dresselhaus, and S. P. Benz, *Phys. Rev. B* **75**, 054514 (2007).
- <sup>15</sup>R. P. Huebener and A. Seher, *Phys. Rev.* **181**, 710 (1969).
- <sup>16</sup>A. Kapitulnik, A. Palevski, and G. Deutscher, *J. Phys. C* **18**, 1305 (1985).
- <sup>17</sup>C. Carballeira, J. Mosqueira, A. Revcolevschi, and F. Vidal, *Phys. Rev. Lett.* **84**, 3157 (2000).
- <sup>18</sup>A. Schmid, *Phys. Rev.* **180**, 527 (1969).
- <sup>19</sup>R. E. Prange, *Phys. Rev. B* **1**, 2349 (1970).
- <sup>20</sup>D. Podolsky, S. Raghu, and A. Vishwanath, *Phys. Rev. Lett.* **99**, 117004 (2007).
- <sup>21</sup>Note the contrast with the conclusions of J. Mosqueira, C. Carballeira, and F. Vidal, *Phys. Rev. Lett.* **87**, 167009 (2001), who reported the vanishing of superconducting fluctuations above  $2 \times T_c$ .
- <sup>22</sup>M. Feigelman (private communication).